Influence of reaction piles on the behaviour of test pile in static load testing

Influence of reaction piles on the behaviour of test pile in static load testing

Pastsakorn Kitiyodom*

Doctoral Student of Graduate School of Kanazawa University, 2-40-20 Kodatsuno, Kanazawa, Ishikawa 920-8667, Japan

Tatsunori Matsumoto**

Department of Civil Engineering, Kanazawa University, 2-40-20 Kodatsuno, Kanazawa, Ishikawa 920-8667, Japan

Nao Kanefusa

Student of Kanazawa University, 2-40-20 Kodatsuno, Kanazawa, Ishikawa 920-8667, Japan

* Correspondence to: Department of Civil Engineering, Kanazawa University, 2-40-20 Kodatsuno, Kanazawa, Ishikawa 920-8667, Japan.

† E-mail: pastsak@nihonkai.kanazawa-u.ac.jp

** Correspondence to: Department of Civil Engineering, Kanazawa University, 2-40-20 Kodatsuno, Kanazawa, Ishikawa 920-8667, Japan.

† E-mail: matsumot@t.kanazawa-u.ac.jp

Influence of reaction piles on the behaviour of test pile in static load testing

Pastsakorn Kitiyodom, Tatsunori Matsumoto and Nao Kanefusa

Abstract: This paper employs a simplified analytical method to investigate the influence of reaction piles on the load-displacement behaviour of the test pile in static load testing. A parametric study is conducted to examine the effects of factors such as pile spacing ratio, pile slenderness ratio and pile soil stiffness ratio. Several soil profiles are considered in this study. The parametric study also includes the cases of static load testing in lateral direction. The correction factors for the initial pile head stiffness obtained from static pile load tests with the use of reaction piles are given in charts. Furthermore, analyses of centrifuge modelling of axially loaded piles are carried out using the simplified analytical method. Good agreements between the test results and the analysis results are demonstrated, and the applicability of the correction factors is verified.

Key words: reaction piles, interaction, initial pile head stiffness, static vertical load testing, static lateral load testing, simplified analytical method.

1. Introduction

Recently, much effort has been done in order to review the foundation design codes. The design methods of foundation structures have been changed from allowable stress design to limit state design or performance based design. In the framework of these new design criteria, estimation of the load-displacement relationship of a pile foundation is a vital issue. The simplest way to obtain the load-displacement relationship of a pile is to conduct an in-situ pile load testing. Many forms of pile load testing are conducted in practice with the aim to obtain a load-displacement relationship for a pile, from which the pile capacity and the pile head stiffness can be estimated. Among them static load testing is the most fundamental. In the test, because heavy loads have to be applied to the test pile, a reaction system which transfers the applied load to the surrounding soil is needed. So, the test may take a variety of forms depending on the means by which the reaction for the loading applied on the test pile is supplied. As an example for the vertical load test of a pile, a test setup in which the reaction is supplied by kentledge, reaction piles, or (vertical or inclined) ground anchors is employed in practice.

In Japan, most static load tests are conducted using reaction piles as the reaction system. The static load test has been regarded to be the most reliable test method, since it is generally believed that a 'true' load-displacement relation of the pile can be directly obtained from the test. It is stated in JGS 1811-2002 (Japanese Geotechnical Society 2002) that as a general rule,

the distances between the centres of the test pile and the reaction piles shall be more than 3 times the maximum diameter of the test pile, and also more than 1.5 meters. Note that the minimum pile spacing had been prescribed as 2.5m in the old version of the JGS standards. However, the minimum pile spacing was reduced to 1.5 m, considering the increase in the use of micropiles in Japan. However, the authors have a question to this common belief, as the interaction between the reaction piles and the test pile may influence the measured pile settlement during the test even for the case where the distances between the centres of the test pile and the reaction piles are greater than 3 times the test pile diameter, as pointed out also by Latotzke et al. (1997), Poulos and Davis (1980), and Poulos (1998). In addition, in Japan at the moment, there are no general rules concerning about the distances between the test pile and the reaction pile in lateral static pile load test standard JSF T32-83 (Japanese Society of Soil Mechanics and Foundation Engineering 1983).

Poulos and Davis (1980) and Poulos (1998) presented workable charts for the correction factors for the initial pile head stiffness obtained from static pile load tests with the use of two reaction piles. However, usually in Japan vertical pile load tests are conducted with four reaction piles. In this work, the influence of the load transfer by four reaction piles on the load-settlement behaviour of the test pile is investigated using a computer program PRAB (Piled Raft Analysis with Batter piles). A parametric study of the influence of reaction piles on the test pile is carried out to investigate the effects of factors such as the pile spacing ratio, the

pile slenderness ratio, the pile soil stiffness ratio, and the soil profile. The influence of reaction piles in lateral pile load tests is also investigated. The correction factors for the initial pile head stiffness obtained from static pile load tests with the use of reaction piles are given in charts for both vertical and lateral load tests. Finally, in order to verify the values of these correction factors, back analyses of the centrifuge modelling of axially loaded piles which were conducted by Latotzke et al. (1997) are carried out.

2. Analysis procedure

The problem is dealt with using a simplified deformation analytical program PRAB that has been developed by Kitiyodom and Matsumoto (2002, 2003). This program is capable of estimating the deformation and load distribution of piled raft foundations subjected to vertical, lateral, and moment loads, using a hybrid model in which the flexible raft is modelled as thin plates and the piles as elastic beams and the soil is treated as springs (Figure 1). Both the vertical and lateral resistances of the piles as well as the raft base are incorporated into the model. Pile-soil-pile, pile-soil-raft and raft-soil-raft interactions are taken into account based on Mindlin's solutions (Mindlin 1936) for both vertical and lateral forces. In addition, an averaging technique suggested by Poulos (1979) is incorporated into the analysis to approximate the interaction between the structure members of a piled raft foundation embedded in non-homogeneous soils. The accuracy of this approximate technique had been

examined in Kitiyodom and Matsumoto (2003) through comparisons with several published solutions and three-dimensional finite element analysis. Note that the solutions from the approximate technique are comparable with the closed form solutions of the interaction given by Mylonakis and Gazetas (1998). When using PRAB to analyze the problem of group of piles without a cap, the soil resistance (soil spring value) at the raft base is set to zero and the stiffness of the raft is set to be very small nearly to zero.

The vertical soil springs, K_z^{Pb}, at the pile base nodes and the vertical soil springs, K_z^{P}, at the pile shaft nodes are estimated using eqs. [1] and [2], respectively, following Lee (1991).

[1] $$K_z^{\mathrm{Pb}} = \frac{4G_{\mathrm{b}}r_{\mathrm{o}}}{1-\nu_{\mathrm{s}}} \times \frac{1}{\left\{1-\exp\left(-h^*/2r_{\mathrm{o}}\right)\right\}}$$

[2] $$K_z^{\mathrm{P}} = \frac{2\pi G \Delta L}{\ln\left(r_{\mathrm{m}}/r_{\mathrm{o}}\right)}$$

[3] $$r_{\mathrm{m}} = 2.5\left[\frac{\sum_{i=1}^{np} G_i L_i}{G_{\mathrm{m}} L}\sqrt{\frac{G_{\mathrm{m}}}{G_{\mathrm{b}}}}\chi L\left(1-\nu_{\mathrm{s}}\right)\right], \quad \chi = 1-\exp\left(1-h/L\right)$$

where

h is the finite soil depth;

h^* is the distance between the pile base and the rigid bed stratum;

r_{o} is the pile radius;

ΔL is the pile segment length;

G_{m} is the maximum soil shear modulus;

G_{b} is the soil shear modulus at the pile base;

ν_s is the Poisson's ratio of the soil;

G_i is the shear modulus of the soil layer i;

L_i is the length of pile embedded in soil layer i

L is the pile embedment length; and

np is the total number of soil layers along the pile embedment length.

The horizontal soil springs, K_x^{Pb} and K_y^{Pb}, at the pile base nodes are estimated using eq. [4].

[4] $$K_x^{Pb} = K_y^{Pb} = \frac{32(1-\nu_s)G_b r_0}{7-8\nu_s}$$

There are many ways to estimate the horizontal soil springs, K_x^P and K_y^P, at the pile shaft nodes. In this paper, the horizontal shaft soil spring values at each pile node are estimated based on Mindlin's solutions which is similar to the solution of the integral method used by Poulos and Davis (1980). The equation becomes

[5] $$K_x^P = K_y^P = \zeta E_s \Delta L$$

[6] $$\zeta = pD / \rho E_s$$

where

E_s is the Young's modulus of the soil;

p is the lateral distributed force acting along a pile element;

D is the pile diameter; and

ρ is the corresponding lateral displacement at each pile node calculated using the

integral equation method. The accuracy of the method for estimation of K_x^{P} and K_y^{P} had been examined in Kitiyodom and Pastsakorn (2002).

In the method, the considered soil profile may be homogeneous semi-infinite, arbitrarily layered and/or underlain by a rigid base stratum. Although the method can easily be extended to include nonlinear response as will be described in Section 5, the emphasis of earlier parametric analyses in Section 3 and Section 4 is placed on the load-displacement relationships of pile foundations where the subsoil still behaves linear-elastically.

In static pile load tests, reaction piles are needed to transfer the load applied to the test pile to the surrounding soil. Since the soil is a continuous material, the load transfer of reaction piles through the soil causes an opposite movement of the test pile because of interaction. As a result, if the displacement of the test pile is measured from a remote point of reference; the measured displacement will be less than the true displacement. In this work, in order to investigate the influence of reaction piles, two types of analysis are carried out. In the first type of analysis, only the test pile is loaded by an applied force, *P*, without the influence of reaction piles (see Figure 2(a) for the case of vertical pile load test and Figure 2(c) for the case of lateral pile load test). The test pile in the first type of analysis is referred to a 'non-influenced test pile' hereafter. The second type of analysis is an idealized in-situ test procedure in which a test pile is loaded by an applied force, *P*, while reaction piles were loaded in the opposite direction by reaction forces as shown in Figure 2(b) and Figure 2(d) for

the case of vertical pile load test and lateral pile load test, respectively. The test pile in the second type of analysis is referred to an 'influenced test pile' hereafter. Note that the diameter of the reaction piles might influence the solution of the problem. However, in this paper considering the circumstance in Japan where the reaction piles are often used as the foundation after the test, only the case of the reaction piles that have the same diameter as the test pile is considered.

The influence of reaction piles will be presented in terms of correction factors, F_c for the case of vertical pile load test and F_c^L for the case of lateral pile load test, which are defined by the ratio of the initial pile head stiffness of the test pile with the use of reaction piles, K_G or K_G^L, to the initial pile head stiffness of non-influenced single pile, K_i or K_i^L (See Figure 3). These correction factors can be applied to the measured pile head stiffsess, K_G or K_G^L, from the test to obtain a truer estimate of the actual pile head stiffness , K_i or K_i^L, of the influenced test pile using eqs. [7] and [8].

[7] $$K_i = K_G / F_c$$

[8] $$K_i^L = K_G^L / F_c^L$$

where

K_i is the initial pile head stiffness for non-influenced test pile for vertical pile load test;

K_G is the initial pile head stiffness for influenced test pile for vertical pile load test;

F_c is the correction factor for vertical pile load test;

K_i^L is the initial pile head stiffness for non-influenced test pile for lateral pile load test;

K_G^L is the initial pile head stiffness for influenced test pile for lateral pile load test; and

F_c^L is the correction factor for lateral pile load test.

For example, in the case of vertical pile load test, the larger value of F_c means that more serious errors arise in the measured settlement of the test pile. The case of $F_c = 1$ means that the measured settlement equals the true settlement of the test pile without influence of the reaction piles.

3. Parametric solutions for vertical pile load testing

Analyses were conducted for single piles and groups of piles embedded in semi-infinite soils, finite depth soils and multi-layered soils. The ranges of the dimensionless parameters were set as 2-10 for the pile spacing ratio s/D, 5-50 for the pile slenderness ratio L/D, 10^2-10^4 for the pile soil stiffness ratio E_p/E_s, and 1-5 for the soil layer depth ratio h/L in the case of pile foundations embedded in finite depth soils. The Poisson's ratio of the soil was set at 0.3 throughout.

3.1 Semi-infinite soil

Figure 4 shows the correction factor $F_c = K_G/K_i$ for the case of floating piles embedded in semi-infinite soils. It can be seen that even for the cases of a pile spacing ratio of 3 which is recommended in the JGS standards, the correction factor may be greater than 2. This means

that the measured settlements in these cases may be less than one half of the true settlements. This can lead to great over-estimation of the initial stiffness of the test piles. Figure 4 also shows that the calculated value of F_c decreases and the distribution of the values becomes narrower as the pile spacing ratio increases, or as the pile soil stiffness ratio decreases. For small values of the pile soil stiffness ratio, the value of F_c increases as the pile slenderness ratio decreases. The opposite trend, the value of F_c increases as the pile slenderness ratio increases, can be found for large values of pile soil stiffness ratio where $E_p/E_s \geq 5000$.

The correction factor $F_c = K_G/K_i$ for the case of floating piles embedded in a semi-infinite soil with the use of 4 reaction piles are compared with the values given by Poulos and Davis (1980) for the case of floating piles embedded in the semi-infinite soil with the use of 2 reaction piles in Figure 5. It can be seen that the trend in the value of F_c for both cases is the same. However, the use of 4 reaction piles, rather than 2, may lead to greater errors in the measured pile head stiffness. As mentioned earlier, vertical pile load tests are usually conducted with four reaction piles in Japan. Therefore, hereafter only the influence of the load transfer by four reaction piles on the load-settlement behaviour of the test pile will be investigated.

3.2 Finite depth soil

In the previous section, the calculated values of F_c were presented for floating piles embedded in semi-infinite homogeneous soils. In practice, soil profiles may be underlain by a

stiff or rigid base soil stratum. In this section, the calculated values of F_c for floating piles and end-bearing piles embedded in finite homogeneous soil layers are presented.

The calculated values of F_c for floating piles embedded in finite homogeneous soil layers are shown in Figure 6. The pile slenderness ratio, L/D, for all cases was set constant at 25. In the figures, the value of F_c for floating piles embedded in semi-infinite soils, h/L = infinity, is also shown. It can be seen that for all cases, the values of F_c for a floating pile embedded in a semi-infinite soil are greater than that of a floating pile embedded in a finite homogeneous soil layer. It can be also seen that the trend in the value of F_c for both cases is the same. That is, the calculated value of F_c decreases and the distribution of the values becomes narrower as the pile spacing ratio increases, or as the pile soil stiffness ratio decreases. The figures also show that the calculated value of F_c for floating piles embedded in finite soil layers decreases as the soil layer depth ratio, h/L, decreases.

Figure 7 shows the values of the correction factor for the case where the soil layer depth ratio of $h/L = 1$ which is the case of end-bearing piles resting on a rigid base stratum. Compared with the value of F_c for the corresponding floating piles embedded in semi-infinite soils or finite homogeneous soil layers, the values of F_c for the case of end-bearing piles resting on a rigid base stratum are smaller. From the figures, it can be seen that the value of F_c for the case of end-bearing piles decreases as the pile spacing ratio increases which is the same trend as the case of floating piles embedded in semi-infinite soils or finite homogeneous

soil layers. However, in the case of end-bearing piles, the value of F_c increases as the pile soil stiffness ratio decreases, which is the opposite trend to that of the calculated results for the case of floating piles. Moreover, the value of F_c increases as the pile slenderness ratio increases.

3.3 Multi-layered soil

Figure 8 shows the calculated values of F_c for the case of floating piles embedded in multi-layered soils. The two soil profiles considered are also indicated in the figure. Compared with the corresponding cases of floating piles embedded in finite homogeneous soil layers which are shown in Figure 6, the values of F_c for the case of floating piles embedded in multi-layered soils are smaller, but the general characteristics of variation of F_c with the pile spacing ratio and the pile soil stiffness ratio remain the same.

4. Parametric solutions for lateral pile load testing

In Section 3, the influence of reaction piles has been presented and discussed for the case of vertical pile load tests. However, in highly seismic areas such as Japan, it is necessary in some cases to conduct a lateral pile load test in order to obtain the pile capacity and pile head stiffness in the lateral direction. In this section, the influence of the load transfer of reaction piles on the load-displacement behaviour of the test pile in the lateral direction is analysed and presented in terms of the correction factor F_c^L. Parametric analyses were conducted for

single piles and groups of piles embedded in semi-infinite soils and finite depth soils. In these analyses, two reaction piles with a constant centre-to-centre distance of 3D were employed, and the distance s* [see Figure 2(d)] was varied. The ranges of the dimensionless parameters were set as 2-10 for the pile spacing ratio s*/D, 5-50 for the pile slenderness ratio L/D, 10^2-10^4 for the pile soil stiffness ratio E_p/E_s, 1-5 for the soil layer depth ratio h/L in the case of pile foundations embedded in finite depth soils, and 0-0.2 for the ratio of the height of loaded point, L_{hp}, to the pile embedment length, L. The Poisson's ratio of the soil was again set at 0.3

4.1 Semi-infinite soil

Figure 9 shows the correction factor $F_c^L = K_G^L/K_i^L$ for the case of piles embedded in semi-infinite soils. It can be clearly seen that the calculated values of F_c^L in the case of the lateral pile load test are smaller than the calculated values of F_c in the case of the vertical pile load test. The figures also show that the trend is the same as in the case of the vertical pile load test, i.e. the value of F_c^L decreases as the pile spacing ratio increases, or as the pile-soil stiffness ratio decreases. In the case of the vertical pile load test, for small values of the pile soil stiffness ratio, the value of F_c increases as the pile slenderness ratio decreases. The opposite trend, the value of F_c increases as the pile slenderness ratio increases, can be found for large values of pile soil stiffness ratio where $E_p/E_s \geq 5000$. However, in the case of the lateral pile load test, this change in trend of the correction factor is not found.

For all of the calculated values of F_c^L shown in Figure 9, it is assumed that the lateral load

was applied at the ground surface level. However, in practice, the lateral load is applied at a point above the ground surface level. In this study, the effects of the distance between the point of applied load and the ground surface level, L_{hp}, was analysed. The calculated values of F_c^L for the case of piles embedded in semi-infinite soils with different heights of the loading point are shown in Figure 10. For all values of the pile soil stiffness ratio, the calculated value of F_c^L decreases as the ratio of the height of loading point to the pile embedment length, L_{hp}/L, increases.

4.2 Finite depth soil

In this section, the calculated values of F_c^L for piles embedded in finite homogeneous soil layers are presented. Figure 11 shows the calculated values of F_c^L for piles with the pile slenderness ratio of L/D = 5. It can be seen that the values of F_c^L in the case of finite homogeneous soil layers are a little bit smaller than the corresponding values of F_c^L in the case of semi-infinite homogeneous soil. The values of F_c^L for piles with the pile slenderness ratio of L/D = 50 are shown in Figure 12. It can be seen that the values of F_c^L are almost the same regardless of h/L. This is thought to be due to the difference in the deformation profile of the laterally loaded pile. Based on the analysis results, in the case of L/D = 5, the pile deformed like a short pile in which all parts of the pile leaned due to the lateral load, and lateral displacement opposite to the loading direction occurred at the pile toe. On the other hand, in the case of L/D = 50, only the top parts of the pile near the loading point deformed

laterally, and no lateral displacement occurred at the pile toe. Thus, in the case of a pile which has a large value of L/D, the value of F_c^L for the pile embedded in semi-infinite homogeneous soil can be used for the pile embedded in finite soil layer.

5. Back analysis of centrifuge model test results

Latotzke et al. (1997) conducted centrifuge model tests on piles in dense sand with an aim to investigate the influence of the load transfer of reaction piles to the soil on the load-settlement behaviour of the test pile. Figure 13 schematically shows two kinds of the tests and the geometrical arrangement of the piles. In the first kind of the test, in order to determine the 'true' load-settlement behaviour of the non-influenced test pile, a single pile alone with a diameter of 30 mm at model scale was modelled in the system. The test pile was pushed down by a hydraulic jack which was fixed on a spreader bar that transferred the reaction forces to the walls of a strong cylinder box with a diameter of 750 mm. In the second kind of the test, one test pile and four reaction piles were employed to model in-situ pile test procedure. By using two hydraulic jacks, the test pile and the group of four reaction piles were loaded separately at the same time. In order to ensure an uniform distribution of the upward load on each reaction pile, the upward loading of the reaction piles was achieved by loading a steel rope that is steered around on several pulleys, and finally hinge-connected on both ends with two reaction piles mounted at a little steel bar. In this test, the least distance

between the centre of the piles was 4.5 times the pile diameter. The dimensions of the reaction piles are equal to the dimensions of the test pile. Applying a g-level of n = 45, a prototype pile with a diameter of D = 1.35 m and an embedded length of L = 9.9 m was modelled. In both kinds of the tests, the model piles were loaded after the centrifuge was spun up to the target speed to produce an acceleration of 45 g.

In this section, back analyses of these centrifuge test results are carried out. The design charts given in earlier sections are also used to estimate the value of the correction factor F_c for these centrifuge data. In the analyses, in order to consider non-linear behaviour of the soil in the analysis, a hyperbolic relationship between shear stress and shear strain, which has been suggested by Randolph (1977), Kraft et al. (1981) and Chow (1986), is employed. The tangent shear modulus of the soil, G_t, is given by

$$G_t = G_{ini}\left(1 - \frac{\tau R_f}{\tau_f}\right)^2 \quad [9]$$

where

G_{ini} is the initial shear modulus of the soil;

τ is the shear stress;

R_f is the hyperbolic curve fitting constant; and

τ_f is the shear stress at failure.

With the tangent shear modulus in eq. [7], the vertical soil spring values, K_z^{Pb}, at the pile base nodes and the vertical soil spring values, K_z^{P}, at the pile shaft nodes (eqs. [1] and [2])

are estimated by means of eqs. [10] and [11].

[10] $$K_z^{Pb} = \frac{4G_{bi}r_o}{1-\nu_s} \times \frac{1}{\{1-\exp(-h^*/2r_o)\}} \times \left(1-\frac{P_b R_f}{P_f}\right)^2$$

[11] $$K_z^{P} = \frac{2\pi G_{ini}\Delta L}{\ln\left(\frac{r_m-\beta}{r_o-\beta}\right)+\left(\frac{\beta(r_m-r_o)}{(r_m-\beta)(r_o-\beta)}\right)}$$

[12] $$\beta = \tau_o r_o R_f / \tau_f$$

where

G_{bi} is the initial shear modulus of the soil at the pile base;

τ_o is the shear stress at the pile-soil interface;

P_b is the mobilized base load; and

P_f is the ultimate base load.

The above vertical soil spring values were incorporated into the computer program PRAB. At high soil strains, yielding of the soil at the pile-soil interfaces occurs and slippage begins to take place. This phenomenon is considered in the program by adopting maximum shaft resistance and maximum end bearing resistance of the vertical soil springs at the pile nodes. In this program, pile-soil-pile interaction is still taken into account based on Mindlin's solutions. Randolph (1994) suggested that the appropriate shear modulus for estimating interaction effects is the 'low-strain' or initial shear modulus, G_{ini}. When the shear strength of the soil is fully mobilized at a particular node, full slippage takes place at the node. Further increases in the load acting on the pile will not increase the soil reaction at that node. Also,

further increases in the loads at the remaining nodes will not cause further increase in displacement of that particular node because of the discontinuity resulting from full slippage taking place. Thus, there is no further interaction through soil between that particular node and the remaining nodes.

In this analysis, in order to model cohesionless sandy soil, a shear modulus linearly increasing with depth was employed. A shaft resistance distribution linearly increasing with depth was also employed and expressed as a function of the shear modulus. The Poisson's ratio of the soil was assumed as 0.3.

Figure 14(a) shows a comparison between the measured load-settlement behaviour of the non-influenced test pile obtained from the centrifuge test and the calculated one. It can be seen from the figure that the calculated load-settlement curve matches very well with the measured curve. For the calculated results in Figure 14(a), a linearly increasing shear modulus profile with $G = 0$ at the ground surface increasing linearly to $G = 52.5$ MN/m^2 at the base of pile was used. The shaft resistance was set as $G/120$, while the maximum value of the base resistance was set at 14 MN/m^2, and the hyperbolic curve fitting constant R_f for the pile shaft nodes and pile base nodes were set at 0.9 and 0.8, respectively. All of these identified values were employed again in the analysis of the influenced test pile. A comparison between the measured load-settlement behaviour of the influenced test pile obtained from the centrifuge test and the calculated one is shown in Figure 14(b). It can be seen from the figure that there

is relatively good agreement between the two results. Focusing on the initial pile head stiffness (initial tangent lines), it can be seen from the figures that the calculated values match very well with the measured values both in the non-influenced test pile and the influenced test pile.

In Figure 15, the calculated and measured values of the correction factor, F_c, at low load are plotted against the total load Q. It can be seen from the figure that the calculated values agree reasonably with the measured value especially in the initial stage.

Moreover, using design chart, for L/D = 9.9/1.35 = 7.3; h/L = 23.4/9.9 = 2.4; s/D = 6.79/1.35 = 5.0; $E_p/(E_s)_{\text{average at 2/3 pile embedment length}}$ = 27000/91 = 296.7; and from Figures 4 and 6, the correction factor, F_c, can be estimated as 1.3. This value is comparable to the measured value. Thus, validity of the proposed values for the correction factor, which have been given in workable charts in earlier sections, is thought to be supported.

6. Conclusions

The influence of the load transfer of reaction piles through the soil on the load-displacement behaviour of the test pile in static load testing was investigated using a simplified analytical program, PRAB. A parametric study was conducted to demonstrate the effects of factors such as pile spacing ratio, pile slenderness ratio, pile soil stiffness ratio and soil profiles for both vertical pile load tests and lateral pile load tests. It was found that the

presence of reaction piles leads to a measured pile head stiffness which is greater than the real (non-influenced) value for both vertical and lateral loading. Correction factors for the initial pile head stiffness obtained from the static pile load tests with the use of reaction piles were given in charts. These values for the correction factors were verified through the back analysis of the centrifuge model test results.

7. Acknowledgement

This study was supported by Grant-in-Aid for Scientific Research (Grant No. 12450188) of Japanese Ministry of Education, Culture, Sports, Science and Technology.

8. References

Chow, Y.K. 1986. Analysis of vertically loaded pile groups. International Journal for Numerical and Analytical Methods in Geomechanics, **10**: 59-72.

Japanese Geotechnical Society 2002. Standards of Japanese geotechnical society for vertical load tests of piles. The Japanese Geotechnical Society, Tokyo.

Japanese Society of Soil Mechanics and Foundation Engineering 1983. JSSMFE standard method for lateral loading test for a pile. The Japanese Society of Soil Mechanics and Foundation Engineering, Tokyo.

Kitiyodom, P., and Matsumoto, T. 2002. A simplified analysis method for piled raft and pile

group foundations with batter piles. International Journal for Numerical and Analytical Methods in Geomechanics, **26**: 1349-1369.

Kitiyodom, P., and Matsumoto, T. 2003. A simplified analysis method for piled raft foundations in non-homogeneous soils. International Journal for Numerical and Analytical Methods in Geomechanics, **27**: 85-109.

Kraft, L.M., Ray, R.P., and Kagawa T. 1981. Theoretical t-z curves. Journal of Geotechnical Engineering, ASCE, **107**(GT11): 1543-1561.

Latotzke, J., König, D., and Jessberger, H.L. 1997. Effects of reaction piles in axial pile tests. *In* Proceedings of the 14th International Conference on Soil Mechanics and Foundation Engineering, Hamburg, Germany, 6-12 September. A.A. Balkema, Rotterdam, Vol. 2, pp. 1097-1101.

Lee, C.Y. 1991. Discrete layer analysis of axially loaded piles and pile groups. Computers and Geotechnics, **11**: 295-313.

Mindlin, R.D. 1936. Force at a point interior of a semi-infinite solid. Physics, **7**: 195-202.

Mylonakis G. and Gazetas G. 1998. Settlement and additional internal forces of grouped piles in layered soil. Géotechnique, **48**(1): 55-72.

Poulos, H.G. 1979. Settlement of single piles in non-homogeneous soil. Journal of Geotechical Engineering, ASCE, **105**(5): 627-641.

Poulos, H.G. 1998. Pile testing-From the designer's viewpoint. *In* Proceedings of the 2nd

International Stanamic Seminar, Tokyo, Japan, 28-30 October. A.A. Balkema, Rotterdam, Vol. 1, pp. 3-21.

Poulos, H.G. and Davis E.H. 1980. Pile Foundation Analysis and Design. Wiley: New York.

Randolph, M.F. 1977. A theoretical study of the performance of piles. Ph.D. thesis, University of Cambridge, Cambridge, U.K.

Randolph, M.F. 1994. Design methods for pile groups and piled rafts. *In* Proceedings of the 13th International Conference on Soil Mechanics and Foundation Engineering, New Delhi, India, 5-10 January. A.A. Balkema, Rotterdam, Vol. 5, pp. 61-82.

9. List of symbols

D	pile diameter
ΔL	pile segment length
E_{p}	pile Young's modulus
E_{s}	soil Young's modulus
F_{c}	correction factor for vertical pile load test
$F_{\mathrm{c}}^{\mathrm{L}}$	correction factor for lateral pile load test
G_{b}	soil shear modulus at the pile base
G_{bi}	initial soil shear modulus at the pile base
G_i	soil shear modulus of the soil layer i
G_{ini}	initial soil shear modulus
G_{m}	maximum soil shear modulus
h	soil layer depth
h^*	distance between the pile base and the rigid base stratum
K_{G}	initial pile head stiffness for influenced test pile for vertical pile load test
K_{i}	initial pile head stiffness for non-influenced test pile for vertical pile load test
$K_{\mathrm{G}}^{\mathrm{L}}$	initial pile head stiffness for influenced test pile for lateral pile load test
$K_{\mathrm{i}}^{\mathrm{L}}$	initial pile head stiffness for non-influenced test pile for lateral pile load test
K_z^{P}	vertical soil springs at pile shaft nodes

K_z^{Pb}	vertical soil springs at pile base nodes
$K_x^{\mathrm{P}}, K_y^{\mathrm{P}}$	horizontal soil springs at pile shaft nodes
$K_x^{\mathrm{Pb}}, K_y^{\mathrm{Pb}}$	horizontal soil springs at pile base nodes
L	pile embedment length
L_{hp}	height of loading point
L_i	pile embedment length in soil layer i
n	centrifuge acceleration level
np	total number of soil layers along the pile embedment length
ν_{s}	Poisson's ratio of the soil
p	lateral distributed force acting along a pile element
P	applied load
P_{b}	mobilized base load
P_{f}	ultimate base load
Q	total load
R_{f}	hyperbolic curve fitting constant
ρ	lateral displacement at each pile node
r_{o}	outer pile radius
s, s^*	pile spacing
τ	shear stress

τ_f shear stress at failure

τ_o shear stress at the pile-soil interface

Figure 1 by Pastsakorn Kitiyodom, Tatsunori Matsumoto and Nao Kanefusa

Fig. 1. Plate-beam-spring modelling of a piled raft foundation.

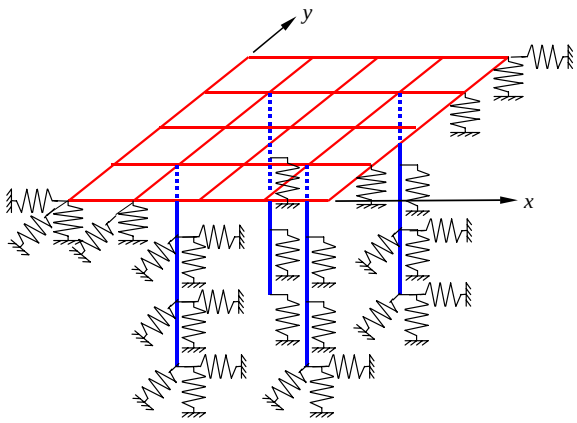

Figure 2 by Pastsakorn Kitiyodom, Tatsunori Matsumoto and Nao Kanefusa

Fig. 2. Cases of analysis.

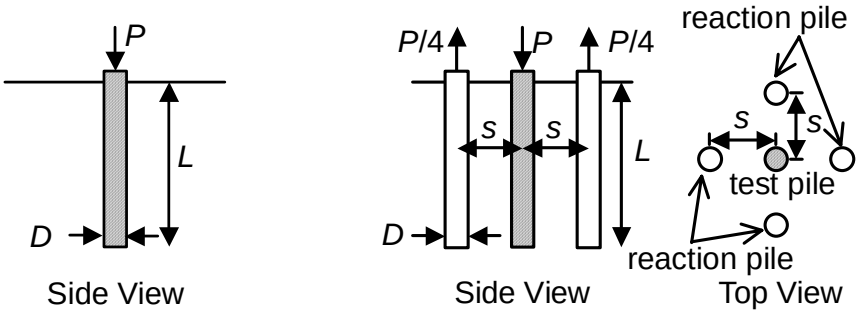

(a) Non-influenced test pile (b) Influenced test pile

Vertical load test

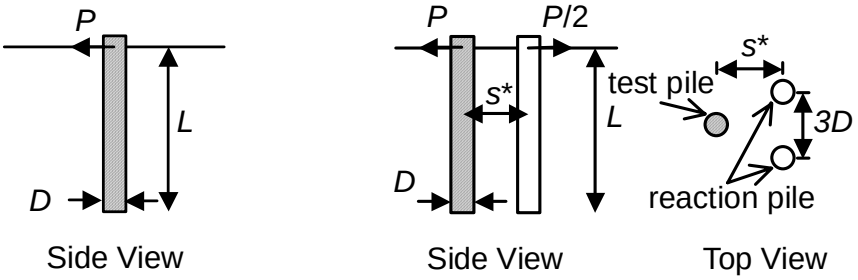

(c) Non-influenced test pile (d) Influenced test pile

Lateral load test

Figure 3 by Pastsakorn Kitiyodom, Tatsunori Matsumoto and Nao Kanefusa

Fig. 3. Illustration for typical load-displacement relations of 'non-influenced test pile' and 'influenced test pile', together with definitions of K_i and K_G.

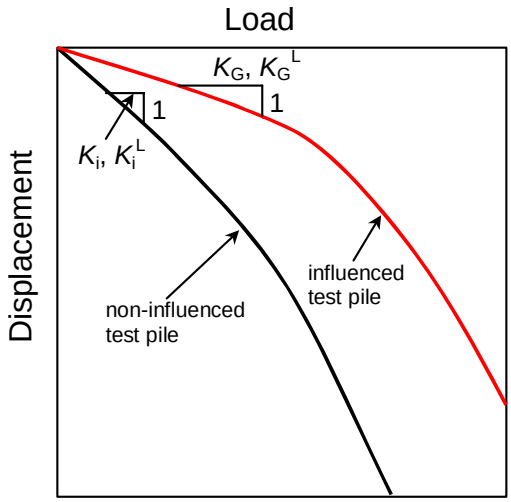

Figure 4 by Pastsakorn Kitiyodom, Tatsunori Matsumoto and Nao Kanefusa

Fig. 4. Correction factor, F_c, for floating piles embedded in semi-infinite soils.

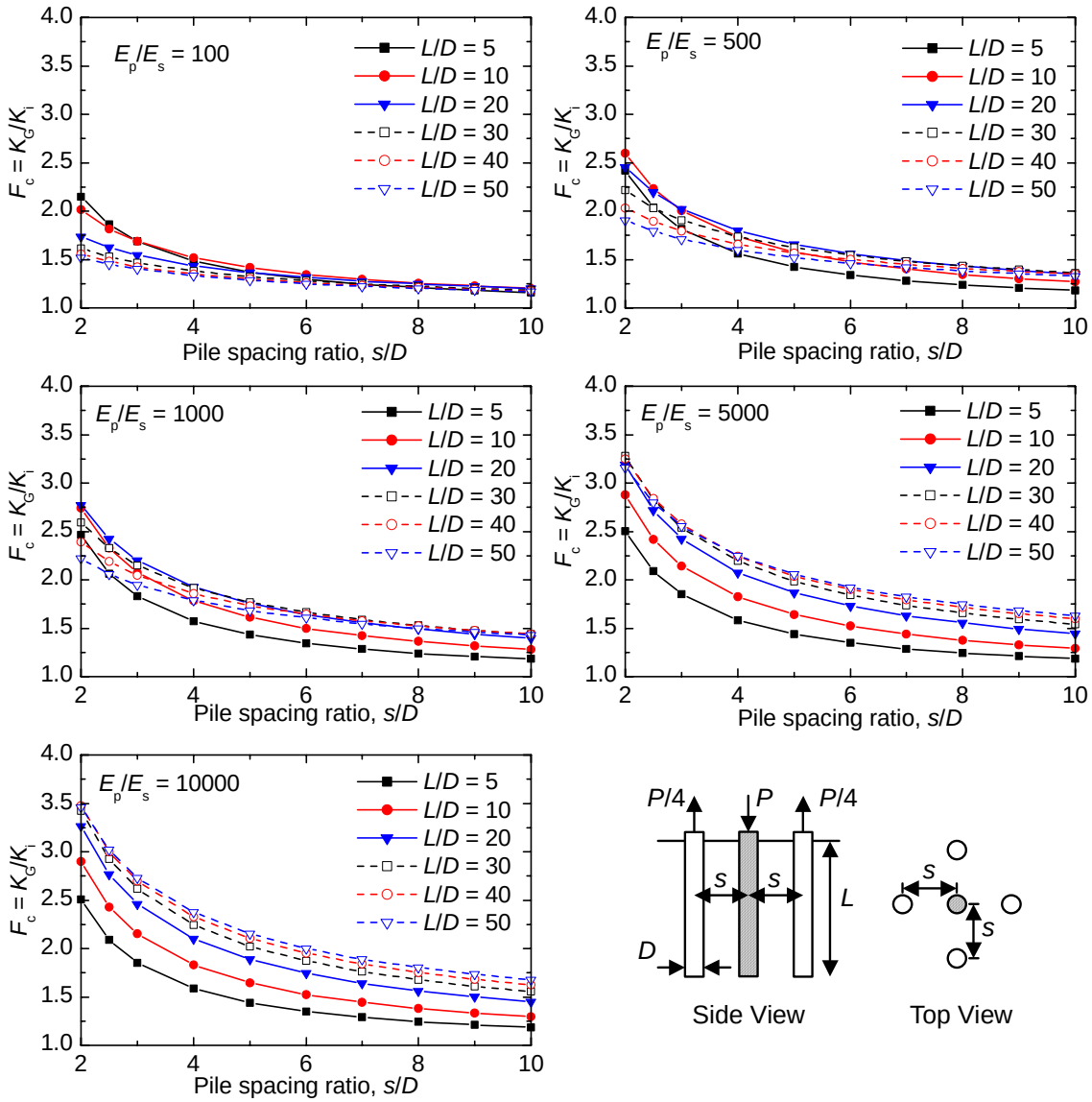

Figure 5 by Pastsakorn Kitiyodom, Tatsunori Matsumoto and Nao Kanefusa

Fig. 5. Comparisons between correction factor, F_c, for floating piles embedded in semi-infinite soils with 4 reaction piles and those with 2 reaction piles.

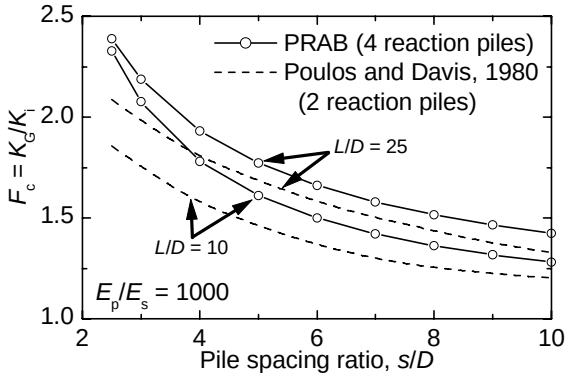

Figure 6 by Pastsakorn Kitiyodom, Tatsunori Matsumoto and Nao Kanefusa

Fig. 6. Correction factor, F_c, for floating piles embedded in finite depth soils with difference in the soil layer depth ratio, h/L (pile slenderness ratio, L/D = 25).

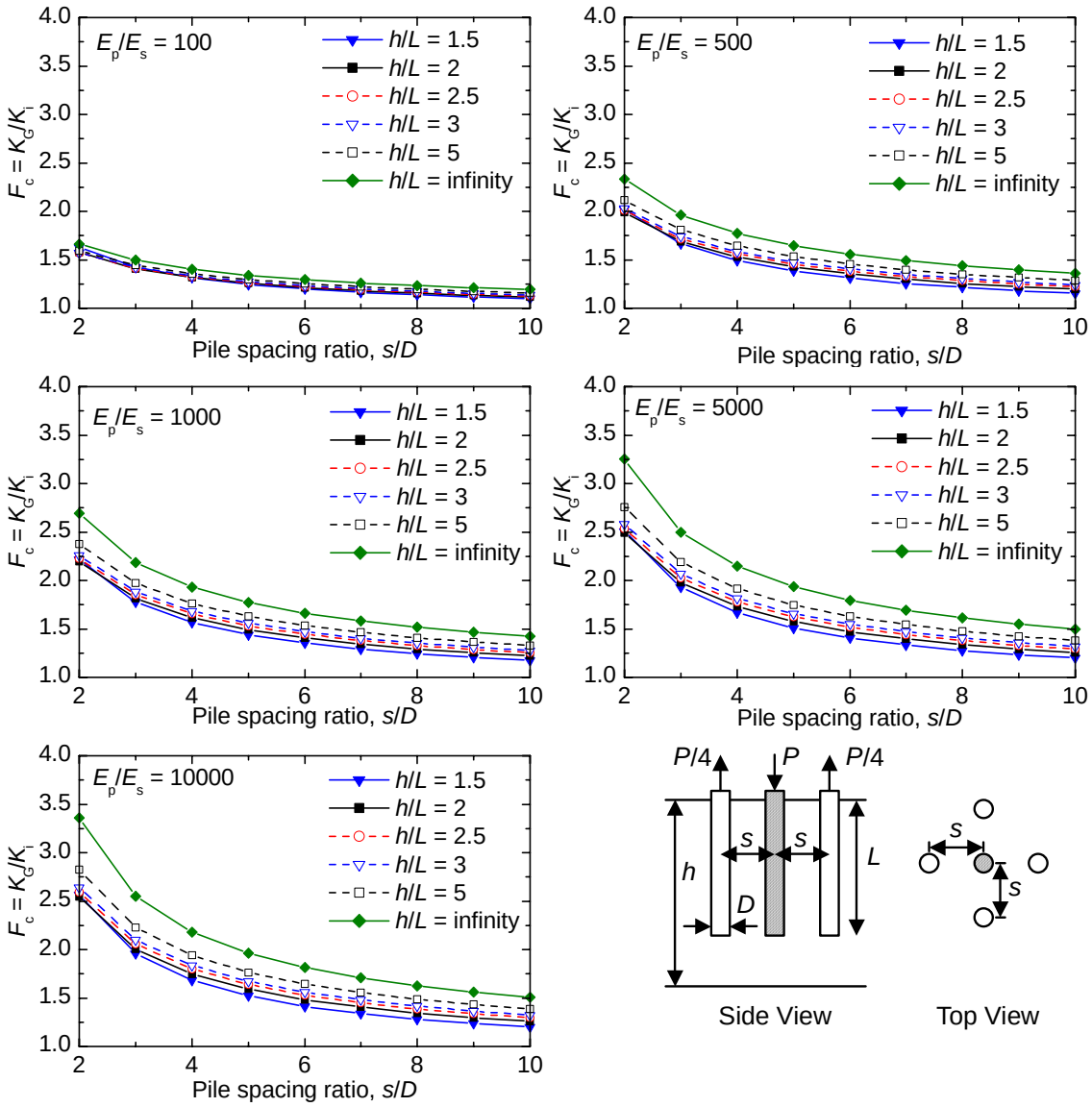

Figure 7 by Pastsakorn Kitiyodom, Tatsunori Matsumoto and Nao Kanefusa

Fig. 7. Correction factor, F_c, for end-bearing piles on rigid base stratum.

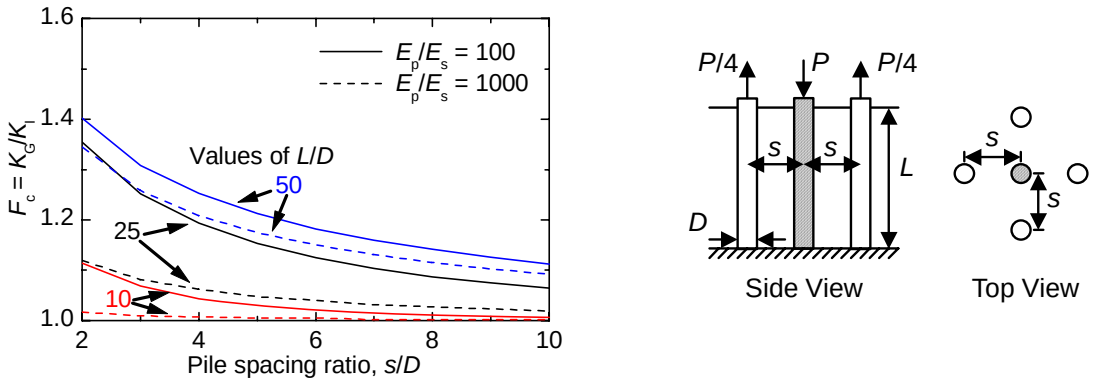

Figure 8 by Pastsakorn Kitiyodom, Tatsunori Matsumoto and Nao Kanefusa

Fig. 8. Correction factor, F_c, for floating piles embedded in multi-layered soils (pile slenderness ratio, L/D = 25).

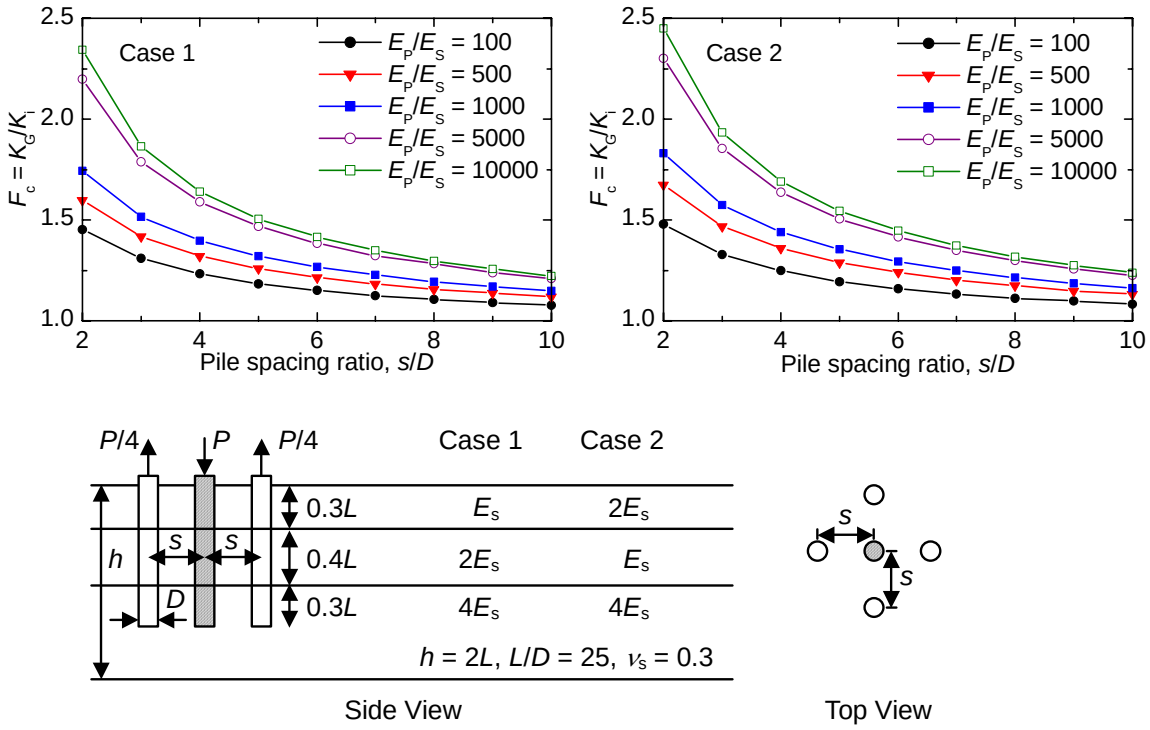

Figure 9 by Pastsakorn Kitiyodom, Tatsunori Matsumoto and Nao Kanefusa

Fig. 9. Correction factor, F_c^L, for piles embedded in semi-infinite soils.

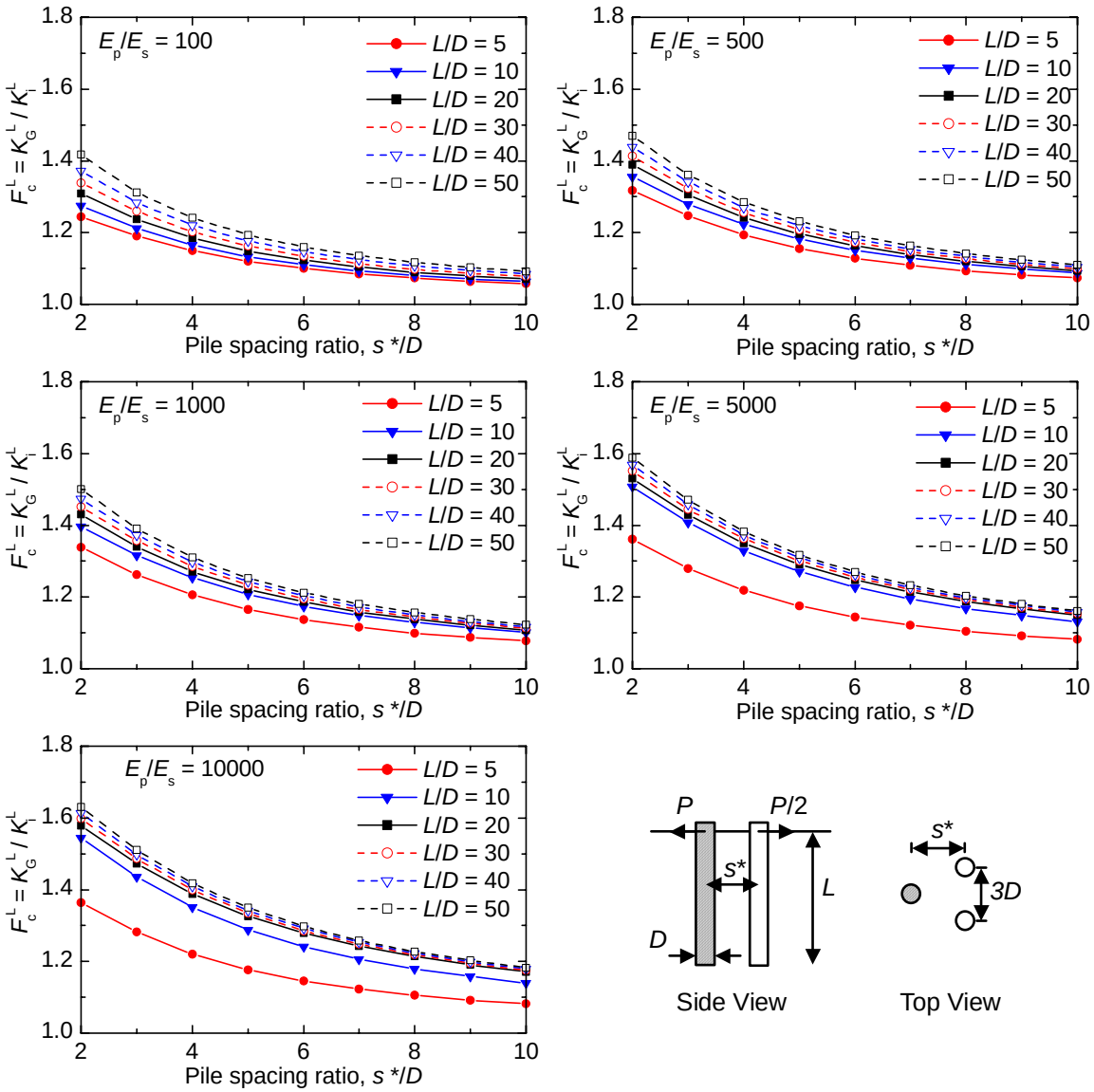

Figure 10 by Pastsakorn Kitiyodom, Tatsunori Matsumoto and Nao Kanefusa

Fig. 10. Correction factor, F_c^L, for piles embedded in semi-infinite soils with different heights of loading point (pile slenderness ratio, L/D = 25).

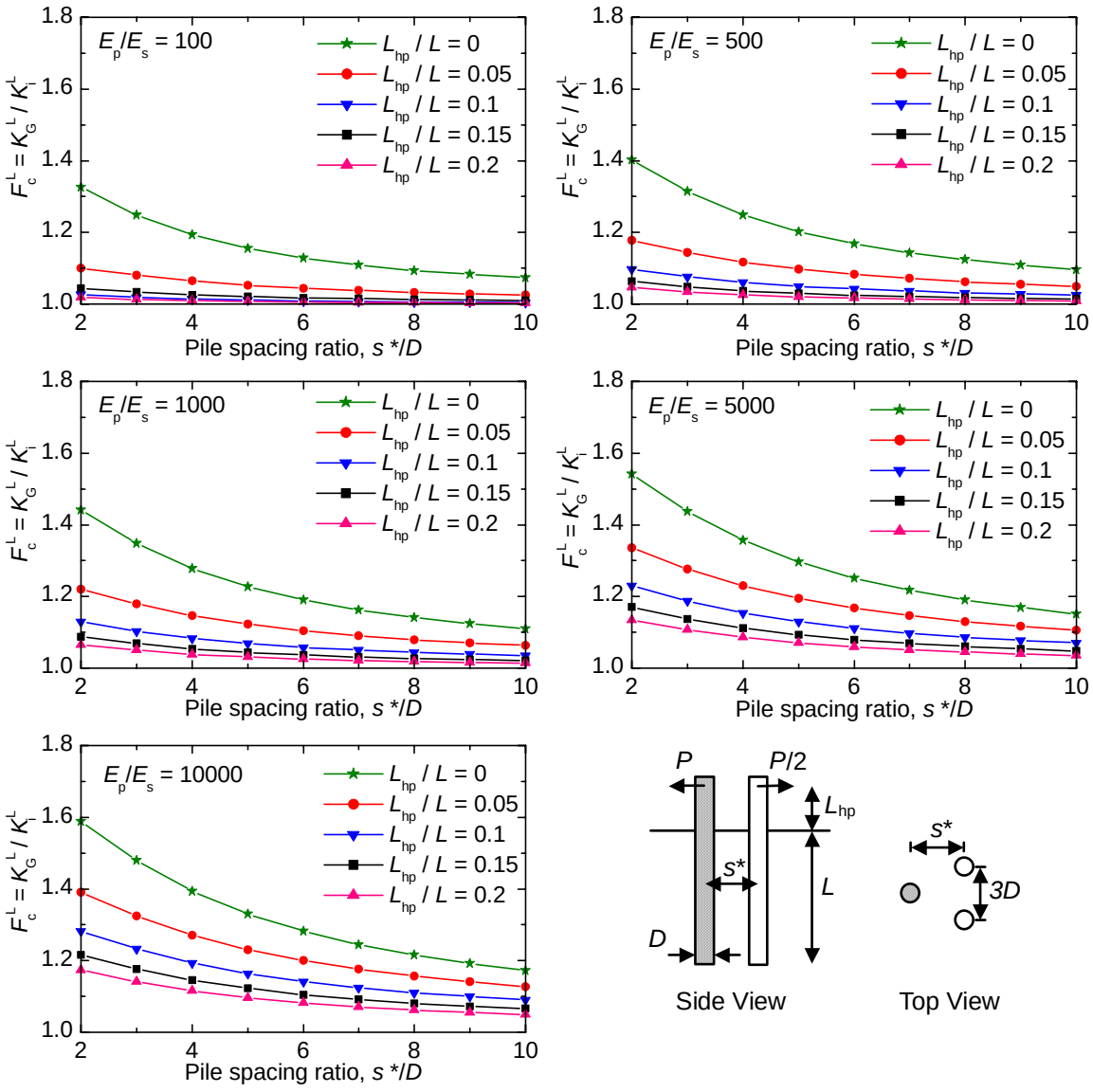

Figure 11 by Pastsakorn Kitiyodom, Tatsunori Matsumoto and Nao Kanefusa

Fig. 11. Correction factor, F_c^L, for piles embedded in finite depth soils with difference in the soil layer depth ratio, h/L (pile slenderness ratio, L/D = 5).

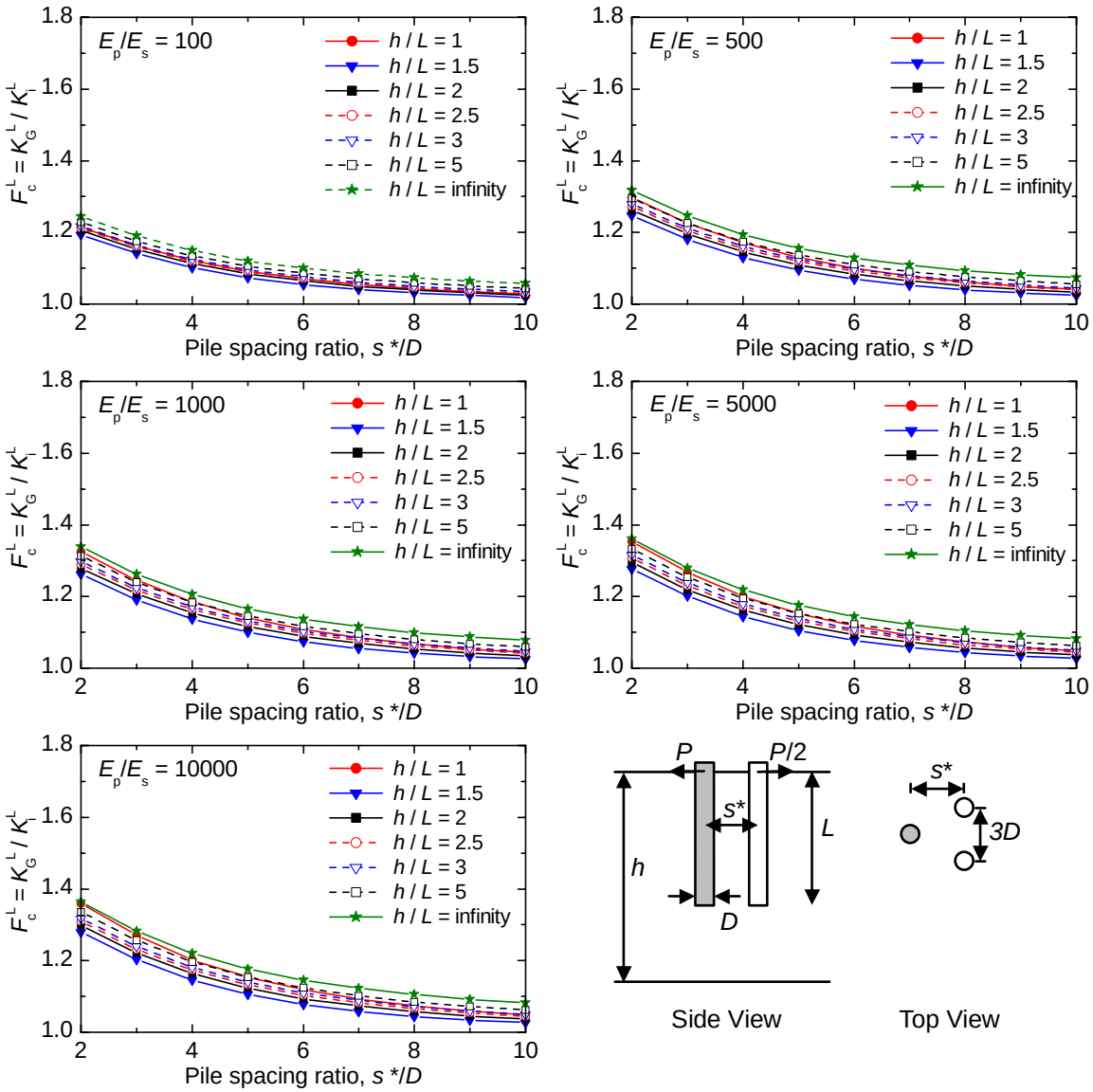

Figure 12 by Pastsakorn Kitiyodom, Tatsunori Matsumoto and Nao Kanefusa

Fig. 12. Correction factor, F_c^L, for piles embedded in finite depth soils with difference in the soil layer depth ratio, h/L (pile slenderness ratio, L/D = 50).

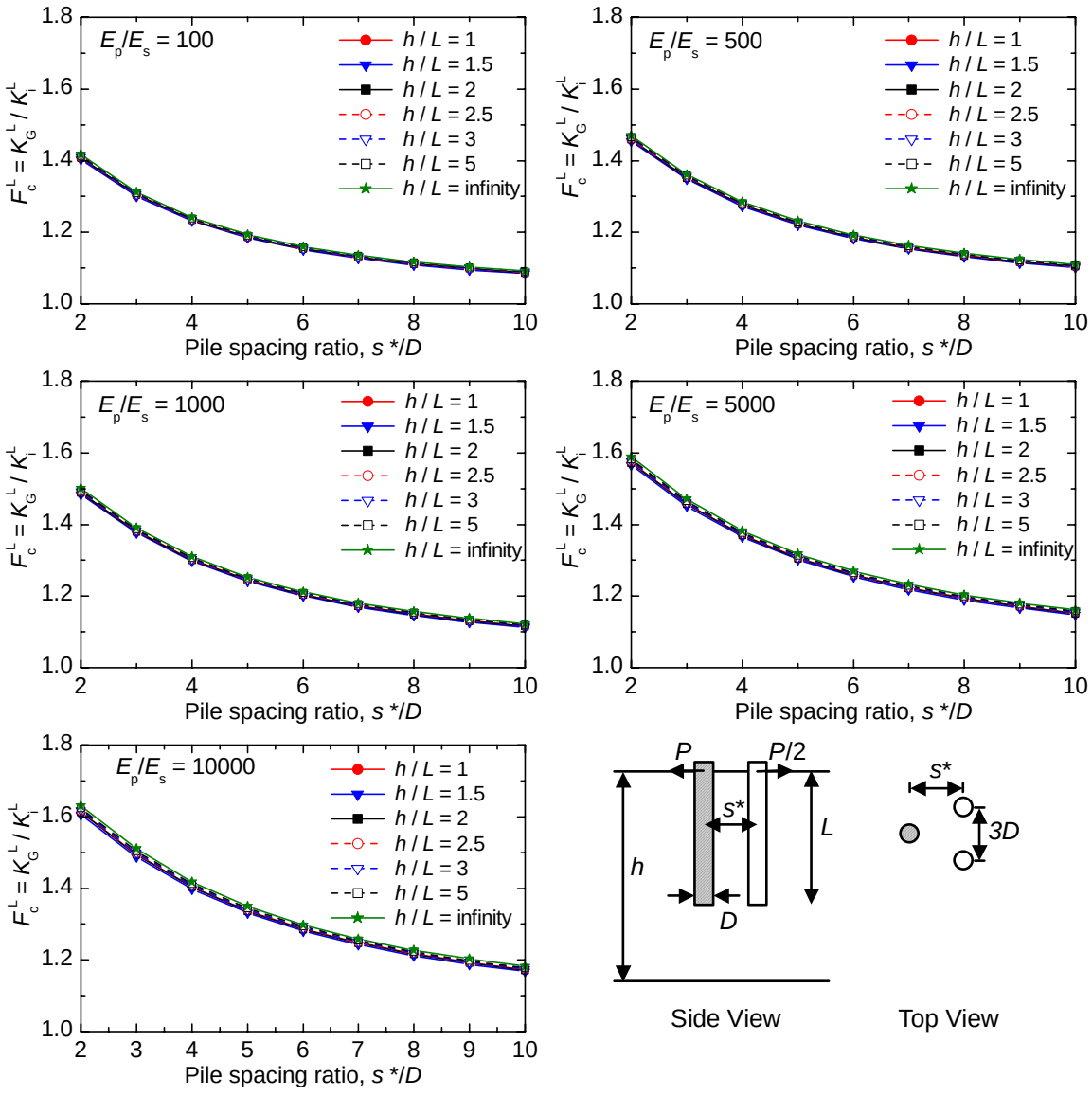

Figure 13 by Pastsakorn Kitiyodom, Tatsunori Matsumoto and Nao Kanefusa

Fig. 13. Two kinds of centrifuge model tests.

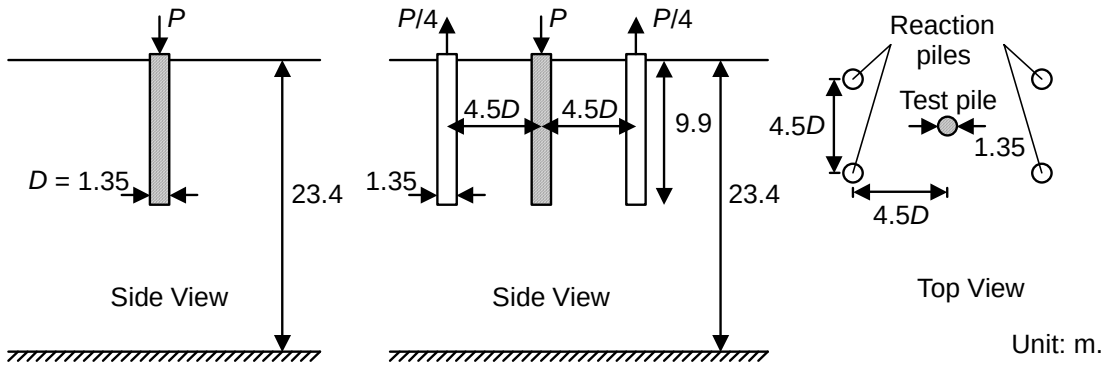

(a) First (non-influenced test pile)

(b) Second (influenced test pile)

Figure 14 by Pastsakorn Kitiyodom, Tatsunori Matsumoto and Nao Kanefusa

Fig. 14. Back analysis results.

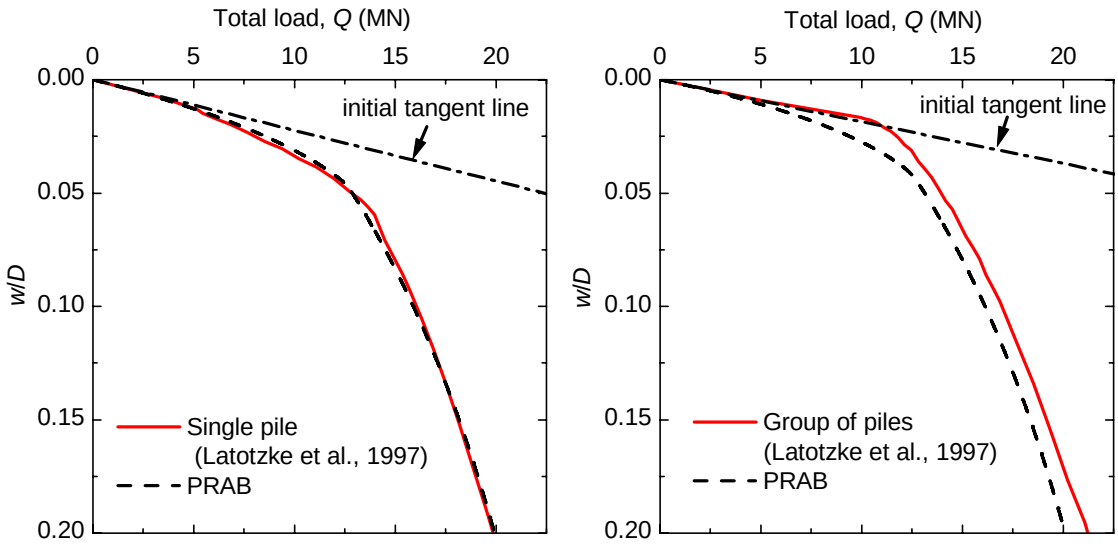

(a) Non-influenced test pile (b) Influenced test pile

Figure 15 by Pastsakorn Kitiyodom, Tatsunori Matsumoto and Nao Kanefusa

Fig. 15. Calculated and measured values of the correction factor.